AN EXPERIMENTAL DETERMINATION OF THE MOTION OF A VORTEX SHEET IN THE WAKE OF AN ISOLATED TWO-BLADED HOVERING MODEL HELICOPTER ROTOR

A THESIS

Presented to

the Faculty of the Graduate Division

by

James Irvin Scott

In Partial Fulfillment

of the Requirements for the Degree

Master of Science in Aeronautical Engineering

Georgia Institute of Technology

September, 1958

"In presenting the dissertation as a partial fulfillment of the requirements for an advanced degree from the Georgia Institute of Technology, I agree that the Library of the Institution shall make it available for inspection and circulation in accordance with its regulations governing materials of this type. I agree that permission to copy from, or to publish from, this dissertation may be granted by the professor under whose direction it was written, or, in his absence, by the dean of the Graduate Division when such copying or publication is solely for scholarly purposes and does not involve potential financial gain. It is understood that any copying from, or publication of, this dissertation which involves potential financial gain will not be allowed without written permission.

_____

/

7A
12R

AN EXPERIMENTAL DETERMINATION OF THE MOTION OF A VORTEX SHEET IN THE WAKE OF AN ISOLATED TWO-BLADED HOVERING MODEL HELICOPTER ROTOR

Approved:

Robin B. Gray

Walter Castles, Jr.

Thomas W. Jackson

Date Approved by Chairman: October 3 1958

ACKNOWLEDGEMENTS

The author wishes to express his appreciation to Doctor Robin B. Gray for suggesting the topic and for his invaluable assistance. The author also wishes to thank Professor Walter Castles, Jr. and Doctor Thomas W. Jackson for their review and criticism of the work.

TABLE OF CONTENTS

LIST OF TABLES

LIST OF FIGURES

LIST OF SYMBOLS

a Blade element lift curve slope, per radian

C_T Rotor thrust coefficient, $C_T = \dfrac{T}{\rho \pi \Omega^2 R^4}$

C_Q Rotor torque coefficient, $C_Q = \dfrac{T}{\rho \pi \Omega^2 R^5}$

r Blade element radius, ft

R Rotor radius, ft

T Rotor thrust, lbs

v_i Normal component of induced velocity at wake vortex sheet element, positive downward, ft/sec

$\bar{v}_i$ Average, or momentum, value of the normal component of induced velocity, positive downward, ft/sec,

$\bar{v}_i = \Omega R \sqrt{\dfrac{C_T}{2}}$

Z Distance measured perpendicular to rotor plane, positive downward, ft

θ Blade element pitch angle, measured between zero lift chord line and rotor plane, degrees

ρ Mass density of air, slugs/ft^3

ψ Azimuth angle of rotor blade measured clockwise from line of smoke probes, degrees

Ω Rotor angular velocity, radians/sec

SUMMARY

The general configuration and movement of a vortex sheet in the wake of an isolated two-bladed hovering model helicopter rotor was determined experimentally to learn more about the flow patterns in the wake of a lifting rotor.

The model rotor was of the "teetering" type. The blades, which had an NACA 43015 airfoil section, were four feet in diameter with a 2:1 taper ratio. The blades operated at a constant blade pitch angle of nine degrees in the speed range of 400-500 rpm.

The flow patterns were determined by means of a smoke visualization technique and motion picture photography. Ten smoke probes were spaced on a wire extending radially and six inches above the plane of the rotor. With the smoke probes operating in succession, motion pictures were made of the path taken by a smoke plume through the rotor wake. A superposition of the results of the smoke visualization studies provided the general configuration and movement of a vortex sheet together with the path and normal component of induced velocity at the vortex sheet elements.

It was found that the length of a cross-section of the vortex sheet in a radial plane increases as the sheet moves through the wake. A nonlinear increase in the normal component of induced velocity of

the vortex sheet elements with an increase in radius, coupled with a nonlinear radial movement inboard causes the outer portion of the vortex sheet to move down through the wake faster than the inboard portion. There is an apparent rotation of the inboard portion of the vortex sheet in a given radial plane about a moving point on the inboard edge of the sheet. The flow at the plane of the rotor and in the wake was unsteady with no discernible periodicity; hence, the results of this report which represents a superposition of smoke studies not taken simultaneously is more qualitative than quantitative in nature. It appears from the results of this investigation that further study and experimentation is warranted.

A quantitative study of the flow patterns in the wake of a lifting rotor would be possible if an entire radial cross-section of the vortex sheets could be photographed with sufficient clarity for an analysis, particularly near the wake periphery. Consideration should be given in future experiments of this nature to the use of colored smoke and color photography which would provide a means of distinguishing the individual smoke plumes when operating simultaneously.

CHAPTER I

INTRODUCTION

A quantitative picture of the flow in the wake of a lifting rotor is required for helicopter force analysis. There has been considerable theoretical and experimental investigation of the air-flow patterns about lifting rotors and the results have proved adequate for many types of helicopter analysis. Very little work has been done relative to the vortex sheets in the wake and their effect on the flow pattern. One of the most recent works in this field by Gray (1)* was an analytical and experimental determination of the motion of the helical vortex shed from the tip of a model rotor together with the approximate position of the vortex sheet.

The purpose of this study was to learn more of the flow pattern in the wake of a lifting rotor by an experimental determination of the position, shape and movement of a vortex sheet in the wake. This was accomplished by means of an air-flow smoke visualization technique and motion picture photography.

Air-flow visualization studies of wake patterns have taken many forms such as the photography of balsa wood dust. Smoke was chosen

---

*Numbers in parentheses refer to items in the bibliography.

as the indicating material for this experiment because of the desirable characteristics of being easily produced, photogenic, and most important, having negligible mass. It would appear that an indicating material such as smoke would be better than balsa dust which has an average free-fall velocity in air of approximately one foot per second, as stated in (2), and thus would affect any quantitative analysis of low velocity flow patterns such as used in this investigation.

CHAPTER II

EQUIPMENT AND INSTRUMENTATION

Model rotor blades.--The model rotor was of the "teetering" type, having blades constructed with a steel leading edge, a laminated walnut trailing edge, and a square tip. The blades were of airfoil contour from a radius of 4.50 inches out and had the following characteristics:

Diameter	48 inches
Blade section (no twist)	NACA 43015
Blade chord	
root chord (extended)	3.016 inches
tip chord	1.508 inches
Taper ratio	2:1

The blade collective pitch could be manually preset from zero to ten degrees.

Rotor test mount.--The rotor hub was mounted on an aluminum shaft which was supported and contained within two hollow aluminum tubes as shown in Figure 1. The outer aluminum tube was flanged and bolted to a structural support rigidly suspended from the ceiling. The rotor blades were thus positioned in the center of a closed room 16 feet wide, 43 feet long, and 11 feet high. As shown in Figure 2, a belt drive from

the motor to the hub pulley rotated the inner tube and the rotor shaft. The rotor shaft was driven through a ball bearing and slip universal joint assembly keyed to the rotor shaft. A beam strain-gage supported the weight of the rotor shaft assembly. An aluminum support diaphragm acted as a centering guide for the rotor shaft. The effect of the diaphragm on the vertical movement of the shaft was considered negligible. The pitch adjustment yoke provided the adjusting linkage for the blade pitch angle and also served as a flapping stop. Power was supplied by a one-half horsepower, 24-volt, direct current aircraft motor, as shown in Figure 3, through a rubber timing belt. This motor was free to rotate against a beam strain-gage which measured the torque. As shown in Figure 4, a rectifier operating from a 220-volt commercial power source supplied the field of the generator and the field of the driving motor. A one horsepower, three phase, induction motor operating from a 220-volt commercial power source operated the 24-volt direct current generator. The voltage supplied by the rectifier to the field of the generator was regulated through a 96 ohm rheostat which in turn regulated the output of the generator to the armature of the driving motor. By this means the rpm of the rotor could be varied from a low speed for calibration to a higher speed for conducting the tests. The output and field voltage of the generator and the field voltage of the driving motor were monitored through voltmeters in the circuit. The rpm of the rotor blades was measured by means of a commutator

mounted on the hub pulley. The thrust and rpm of the rotor blades and the torque of the driving motor were recorded by an oscillograph as shown in Figures 5 and 6. A blade azimuth position indicator which consisted of a pointer and a dial was mounted on the rotor test mount. The pointer was keyed to the shaft of a selsyn motor. The selsyn generator was driven through a two to one gear reduction ratio by an idler shaft operating from the timing belt.

Smoke source. --Ten smoke probes were suspended on a wire extending radially and six inches above the plane of the rotor. The most inboard probe was located six inches from the axis of the rotor shaft. The remaining probes were placed at three inch intervals. A probe consisted of an eye dropper loosely packed with cotton with a wick in the tip. Titanium tetrachloride introduced into the dropper saturated the cotton and was exposed to the atmosphere through the wick resulting in a dense plume of smoke.

Camera and lighting. --A 16mm movie camera photographed a radial cross section of the wake of the rotor blades materialized by the smoke. The camera was positioned eight feet from the cross section of the wake. The optical axis of the camera was normal to the center of the cross section of the wake. The camera was equipped with a 16mm, f 1.6 lens and operated at 64 frames per second. Two banks of four 300-watt reflector flood lights each, placed on the floor, illuminated the front and back of the cross section of the wake.

CHAPTER III

PROCEDURE

Calibration. --The instrumentation was given a static calibration prior to the installation of the rotor blades. The diaphragm supported the weight of the rotor shaft assembly less blades. Known weights were suspended from the bottom of the rotor shaft and a calibration record was made on the oscillograph. The maximum weight added during the calibration corresponded to the weight of the rotor blades. A calibration record reflected a loading and unloading of the beam strain-gage. An average value obtained from this record was used to convert the thrust strain-gage data to thrust. The thrust produced by the blades during the tests had the effect of unloading the strain-gage. The torque strain-gage was calibrated by suspending known weights directly from the beam of the strain-gage. Friction torque was determined by hanging weights to the bottom of the shaft which was rotated without blades.

Test procedure. --Immediately before and after each test run, an oscillograph recording was made while the blades were rotating at a very low rpm to establish the zero thrust. Titanium tetrachloride was introduced into one of the smoke probes. The rotor blades were then

brought up to test speed (400-500 rpm). When the flow of smoke through the rotor blades appeared to have reached a steady state, the camera and oscillograph were operated simultaneously for a one to two second period. This procedure was repeated for each smoke probe. For reference, the smoke probes were numbered one through ten starting with the most inboard probe. Initially it was planned to have all of the smoke probes operating simultaneously; however, when this was tried the paths of the most outboard smoke plumes could not be clearly distinguished from one another, as shown in Figure 7.

A blade pitch angle of nine degrees was set by means of the pitch adjustment yoke. All of the tests were run with the same blade pitch angle.

Reduction of data. --The general configuration and movement of a vortex sheet element in the wake of the rotor was determined by a frame by frame study of the motion pictures. Each smoke plume materialized an element of the vortex sheet. The elements from each smoke plume were traced in their path through the wake from a one-quarter scale projection of the film. Each frame of the film also indicated the blade azimuth position. A sequence of photographs showing the movement of a vortex sheet element is shown in Figure 8. A typical plot of a vortex sheet element is shown in Figure 9.

From each vortex sheet element plot, the average non-dimensional rectangular coordinates, r/R and Z/R, for each position of the vortex

sheet element in a radial plane in the wake were plotted versus the azimuth angle of the rotor blade measured clockwise from the line of smoke probes, ψ. From this data it was possible to make a superposition of the plots of the individual vortex sheet elements, as shown in Figure 10, irrespective of the differences in rotor speed, Ω, between test runs. The general configuration and movement of the vortex sheet is shown per 90 degrees of blade rotation.

The path of the vortex sheet elements in the wake of the rotor was determined by joining the consecutive vortex sheet elements with a smooth curve as shown in Figure 11.

From Figure 10 and knowing Ω, it was possible to determine the normal component of induced velocity of the vortex sheet elements in the rotor wake as shown in Figure 12. The normal component of the induced velocity at the plane of the rotor was determined by extrapolation to $Z = 0$ from Figure 12. These values are shown in Table 1.

The momentum theory was used to determine a value of C_T with the assumption that the wake is fully developed at $Z/R = 0.75$. From the momentum theory

$$dT = 4\pi\rho\, v_i^2\, r\, dr$$

$$\text{or} \qquad dC_T/dr = v_i^2\, r/4\Omega^2$$

The normal component of induced velocity of the wake vortex sheet element, v_i, evaluated at $Z/R = 0.75$, was determined from Figure 12

and a corresponding value of the vortex element radius, r, was determined from Figure 11. By graphic integration of the above equation, $C_T = 0.00503$.

No evaluation of the thrust and torque strain-gage data to determine an experimental value of C_T and C_Q was possible because of a malfunction of the oscillograph recorder. This fact was not discovered until after the testing apparatus and instrumentation had been disassembled and converted to other uses.

CHAPTER IV

DISCUSSION OF RESULTS

The position of a particular vortex sheet element in Figure 10 and the path of a vortex sheet element in Figure 11 represents only the position and path as determined for the particular sequence of photographs studied. Cognizance must be taken of this fact because the path taken by a particular smoke plume was not steady. There was no apparent periodicity in the radial movement of the smoke plumes in the plane of the rotor. The radial movement of a plume in the plane of the rotor varied from $\pm$ 0.5 inches for No. 1 probe to $\pm$ 3.0 inches for probe Nos. 8 and 9. The plume from No. 10 probe varied $\pm$ 1.5 inches, but on one occasion wafted up and came down through the center of the blade radius, and on another occasion curled under the tip of the blade. No attempt was made to measure the radial oscillations of the smoke plumes in the wake. It is interesting to note that the particular sequence of photographs studied placed the entry of the smoke plume from No. 10 probe at $r = 0.83$ which coincides with the value of the initial wake radius computed by the method of (3). The points of entry into the plane of the rotor represent, with one exception, median points of the radial variations of the individual smoke plumes. No acceptable plot of the smoke plume from probe No. 8 could be obtained and the

plot indicated is not at a median point. It will be noted in Figure 11 that some of the paths of the vortex sheet elements apparently cross. This is caused by the unsteadiness of the flow coupled with the individual analysis of the smoke plumes as explained above, and the fact that there is a rotation of the wake. What has been depicted in Figures 10 and 11 as a two-dimensional flow pattern is actually of a three-dimensional nature and hence some distortion is to be expected. A displacement of the smoke plumes in the tangential direction at the plane of the rotor was noted when observations were made along the blade axis. There was a varying tangential displacement of the smoke plumes in the direction of rotation which was very small at the most inboard station and becoming more pronounced when the plume originated outside of the rotor plane.

From Figure 10 the following general observations can be made concerning the general configuration and movement of the vortex sheet: The length of a cross section of the vortex sheet in a radial plane increases as it moves through the wake. A nonlinear increase in the normal component of induced velocity of the vortex sheet elements with an increase in radius, coupled with a nonlinear radial movement inboard, causes the outboard portion of the sheet to move down through the wake faster than the inboard portion and an apparent rotation of the inboard portion about the most inboard element. Considering only a measurement in the radial direction, the vortex sheet contracts with

the movement through the wake.

The experimental values of the normal component of induced velocity at the plane of the rotor are compared nondimensionally in Table 1 and Figure 13 to the values obtained in (4) for a triangular disk loading, and the values given by the blade element theory of (5). The experimental values indicate that the nondimensional velocity ratio $v_i / \overline{v}_i$ is nonlinear out to a nondimensional blade radius of $r/R = 0.7$ in conformity with the blade element theory and then becomes linear out to a blade radius of $r/R = 0.83$ in the fashion of a triangular disk loading. The experimental values that were plotted in Figure 13 correspond to the probes whose smoke plumes are indicated in solid lines in Figure 11. The relatively satisfactory agreement shown in Figure 13 would indicate that these paths of the vortex elements are shown in their approximate median positions in the wake.

By the methods of (5), $C_T = .00424$ for the blade angle and rotor blades used in this experiment where a value of the blade element lift curve slope per radian, a, equals 5.83 was assumed. Castles (6), using the same rotor blades and θ but with an Λ that was three times greater, was in good agreement with this value of C_T. If the independence of the blade elements is assumed and if a of each blade element may be taken to be two-dimensional, then the difference in Reynold's Number between the experiments recorded in (6) and this experiment would have the effect of increasing the value of the lift

curve slope from the assumed average value of 5.83 to about 7 as indicated in (7). Using the latter value of a in the blade element theory would yield a value of C_T on the order of 0.005 which would be in good agreement with the experimental value determined from the momentum theory of 0.00503.

CHAPTER V

CONCLUSIONS

An experimental study of the general configuration and movement of a vortex sheet in the wake of a hovering lifting rotor indicates that:

1. The length of a cross section of the vortex sheet in a radial plane increases as it moves through the wake.

2. In the plane of the rotor the normal component of induced velocity of the vortex sheet elements is nonlinear out to a nondimensional blade radius of $r/R = 0.7$ and very nearly linear from $r/R = 0.7$ to $r/R = 0.83$.

3. Along any given radius in the wake of the rotor, there is a nonlinear variation in the normal component of induced velocity of the vortex sheet elements.

4. The flow at the plane of the rotor and in the wake was unsteady with no discernible periodicity.

5. Based on the results obtained from this experiment, it appears that further study and experimentation is warranted using the general techniques of this investigation.

CHAPTER VI

RECOMMENDATIONS

To provide a quantitative picture of the flow patterns in the wake of a lifting rotor, it will be necessary to study a series of complete flow patterns. To accomplish this the wake flow pattern should be evaluated from a series of smoke plumes that are operating simultaneously. In any future experiments of this nature, serious consideration should be given to using colored smoke generators and color photography.

If the smoke studies were to be repeated, the smoke probes would be independent of any connection to the rotor test mount, as any vibration of the test mount can cause an interruption of a smooth flow of smoke if the two are linked.

Consideration should be given in any future smoke visualization studies by motion picture photography to making direct measurements from a continuous roll of photographs rather than by the projection methods used.

APPENDIX

Table 1. Summary of Data for a Two-Bladed Rotor in Hovering Flight. $\theta = 9.0^{\circ}$ $\rho = 00221$

Record Number	Probe Number	r/R (1)	κ	$\bar{v}_i$	v_i (2)	$v_i/\bar{v}_i$ (2)	v_i (3)	$v_i/\bar{v}_i$ (3)	v_i (4)	$v_i/\bar{v}_i$ (4)
07022	1	.31	45.5	4.19	2.2	.53	1.93	.46	2.73	.65
07026	2	.38	47.1	4.33	3.5	.81	2.42	.56	3.21	.74
07030	3	.46	46.9	4.31	4.0	.93	2.98	.69	3.62	.84
07034	4	.58	47.8	4.40	4.8	1.09	3.87	.88	4.18	.95
07037	5	.65	46.6	4.29	4.5	1.05	4.15	.97	4.31	1.00
07041	6	.72	46.4	4.27	6.0	1.41	4.61	1.08	4.51	1.06
07045	7	.73	47.4	4.36	5.0	1.15	4.75	1.09	4.60	1.06
07049	8	.71	47.6	4.38	5.2	1.19	4.74	1.08	4.68	1.07
07057	9	.76	49.2	4.53	5.5	1.21	5.16	1.14	4.90	1.08
07061	10	.83	50.4	4.64	6.2	1.34	5.80	1.25	5.21	1.12

(1) Nondimensional radius of smoke plume at rotor plane
(2) Experimental values
(3) By the method of (4)
(4) By the method of (5)

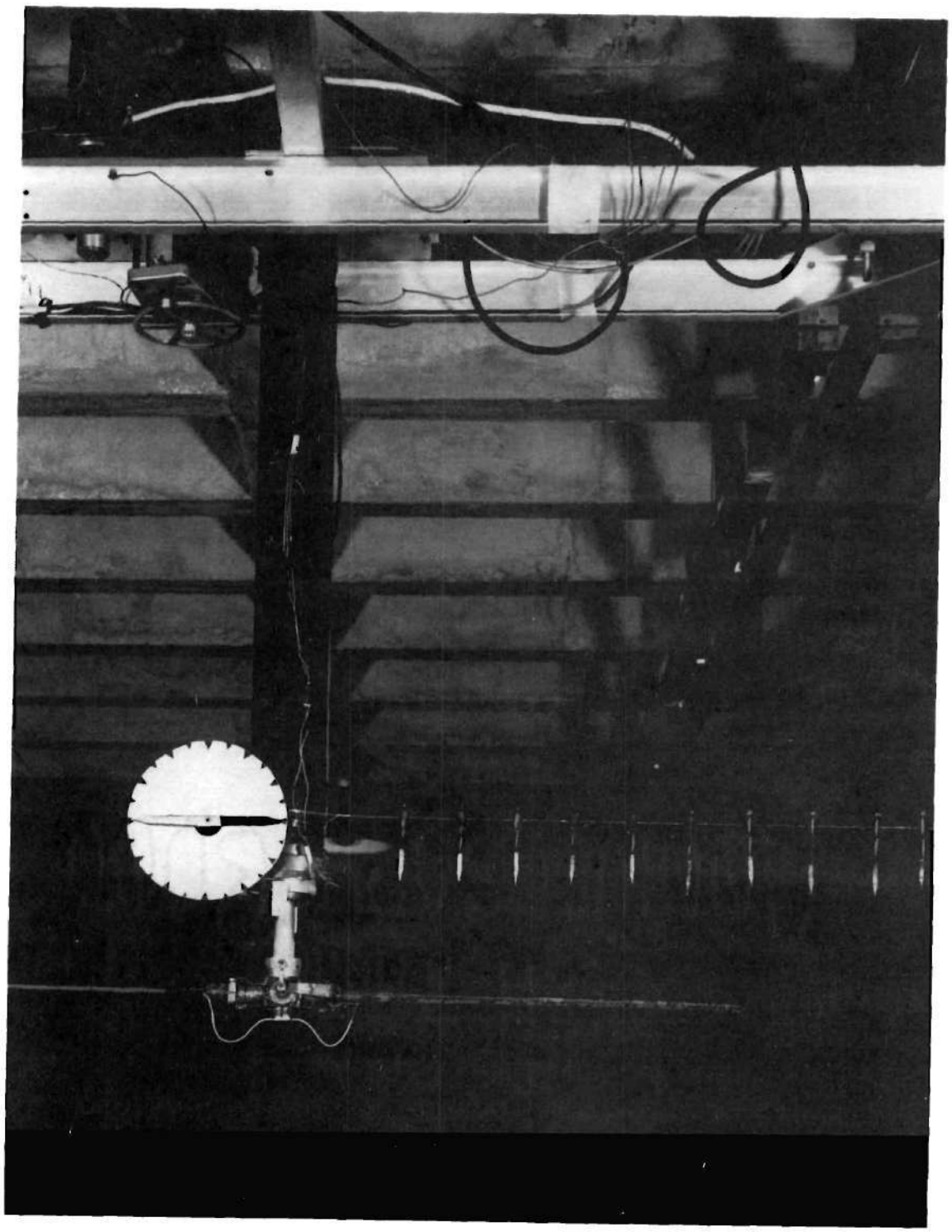

Figure 1. Rotor Test Mount with Blades Attached

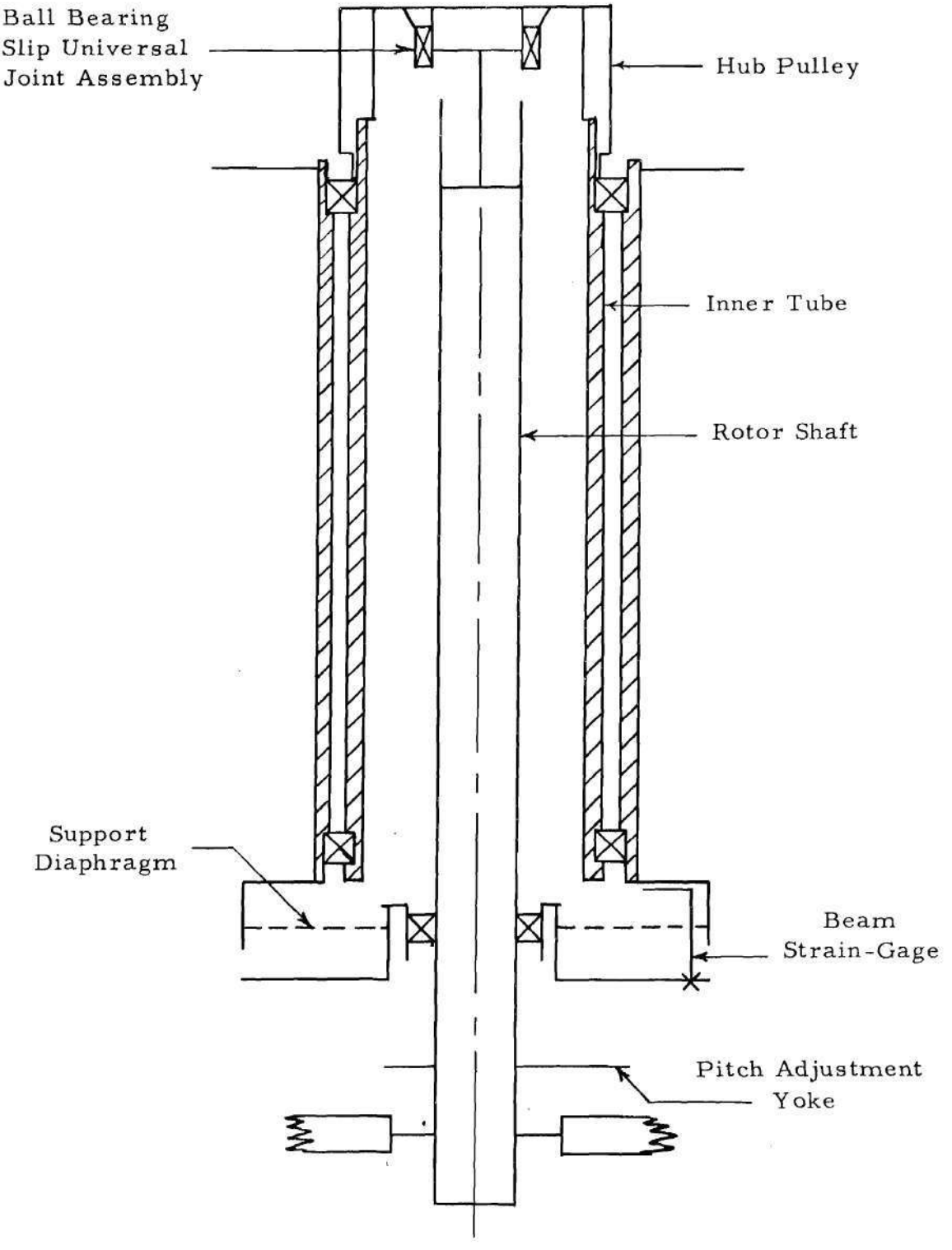

Figure 2. Schematic Drawing of Rotor Test Mount

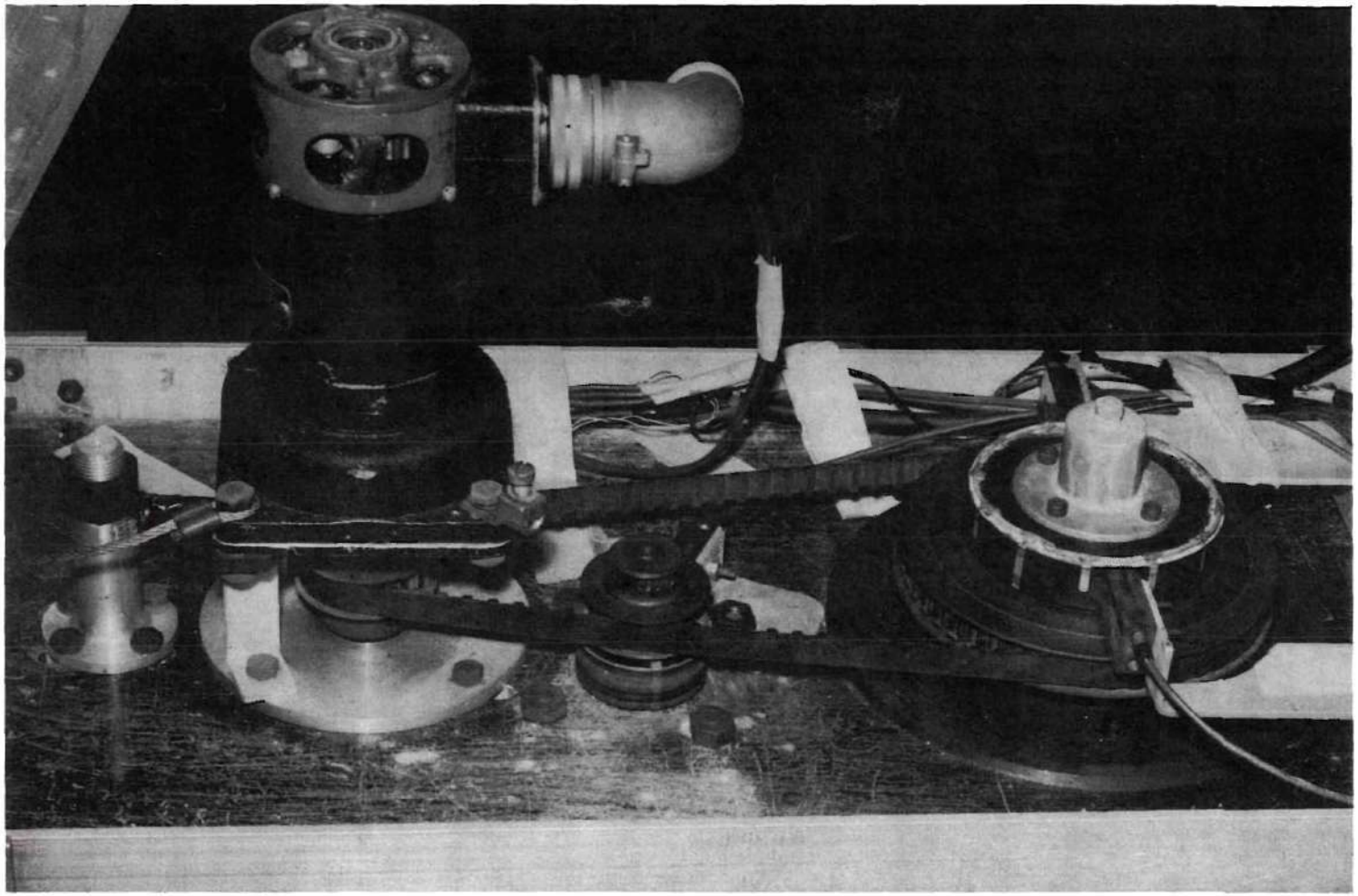

Figure 3. Rotor Test Mount Showing Driving Motor

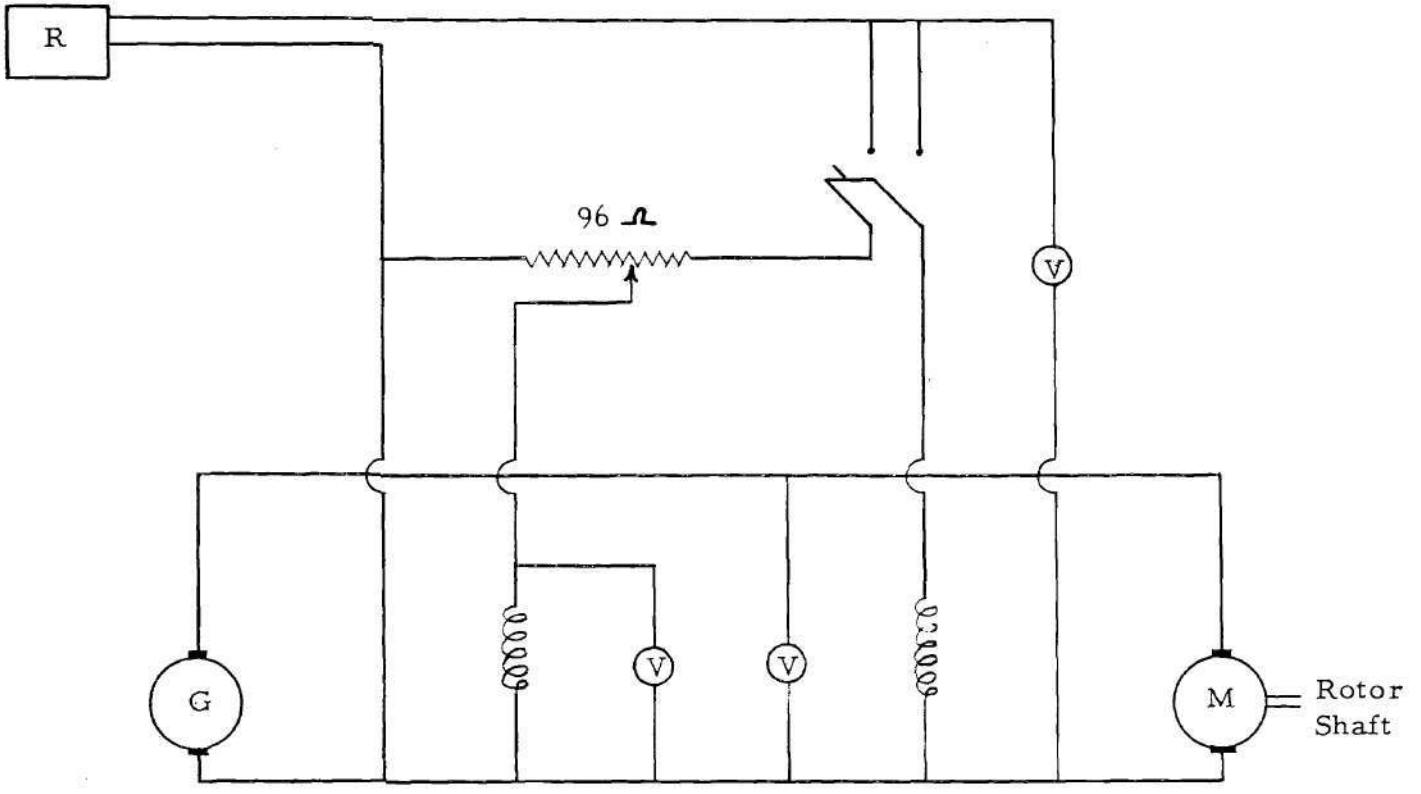

Figure 4. Rotor Test Mount Circuit Diagram

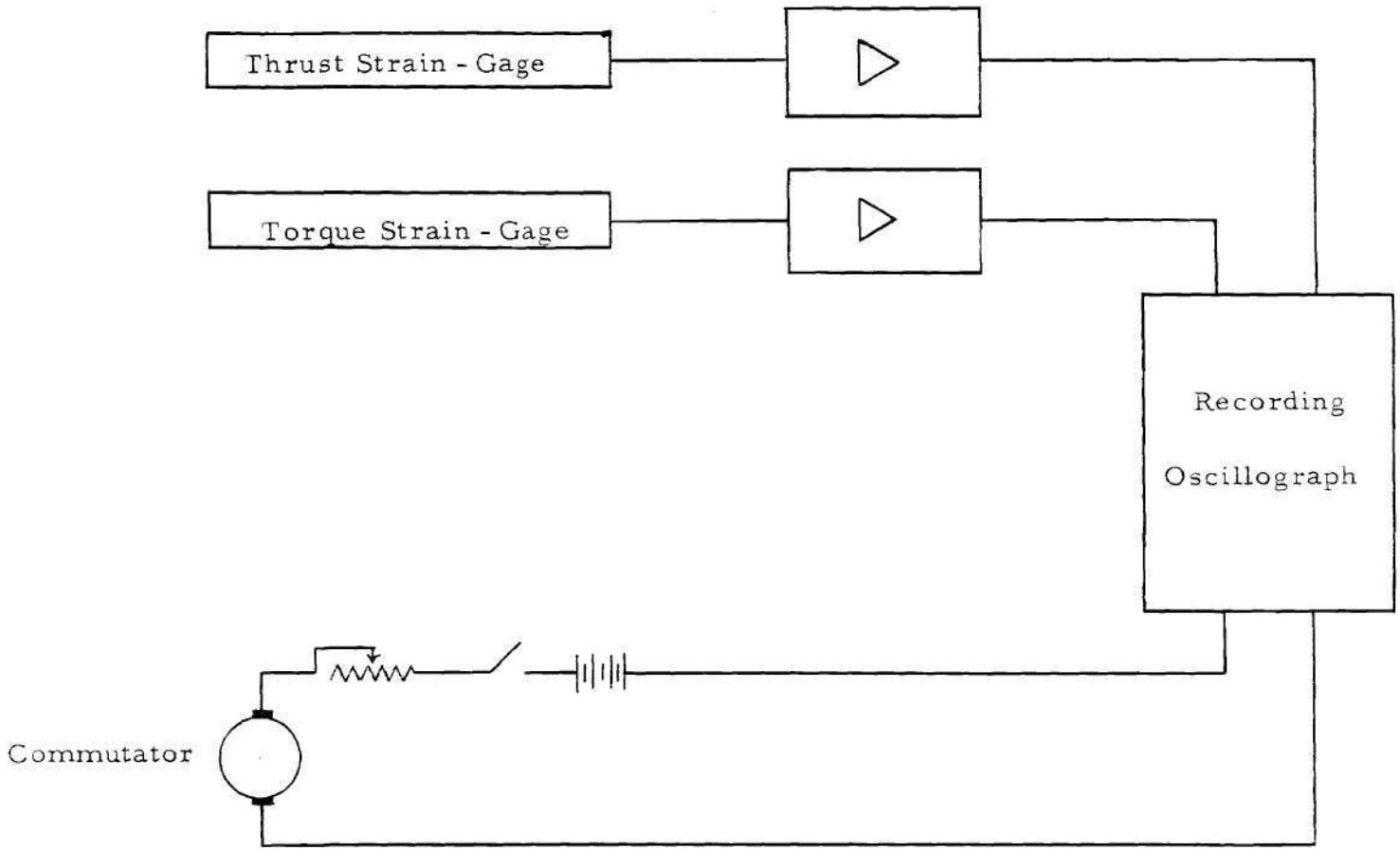

Figure 5. Instrumentation Circuit Diagram

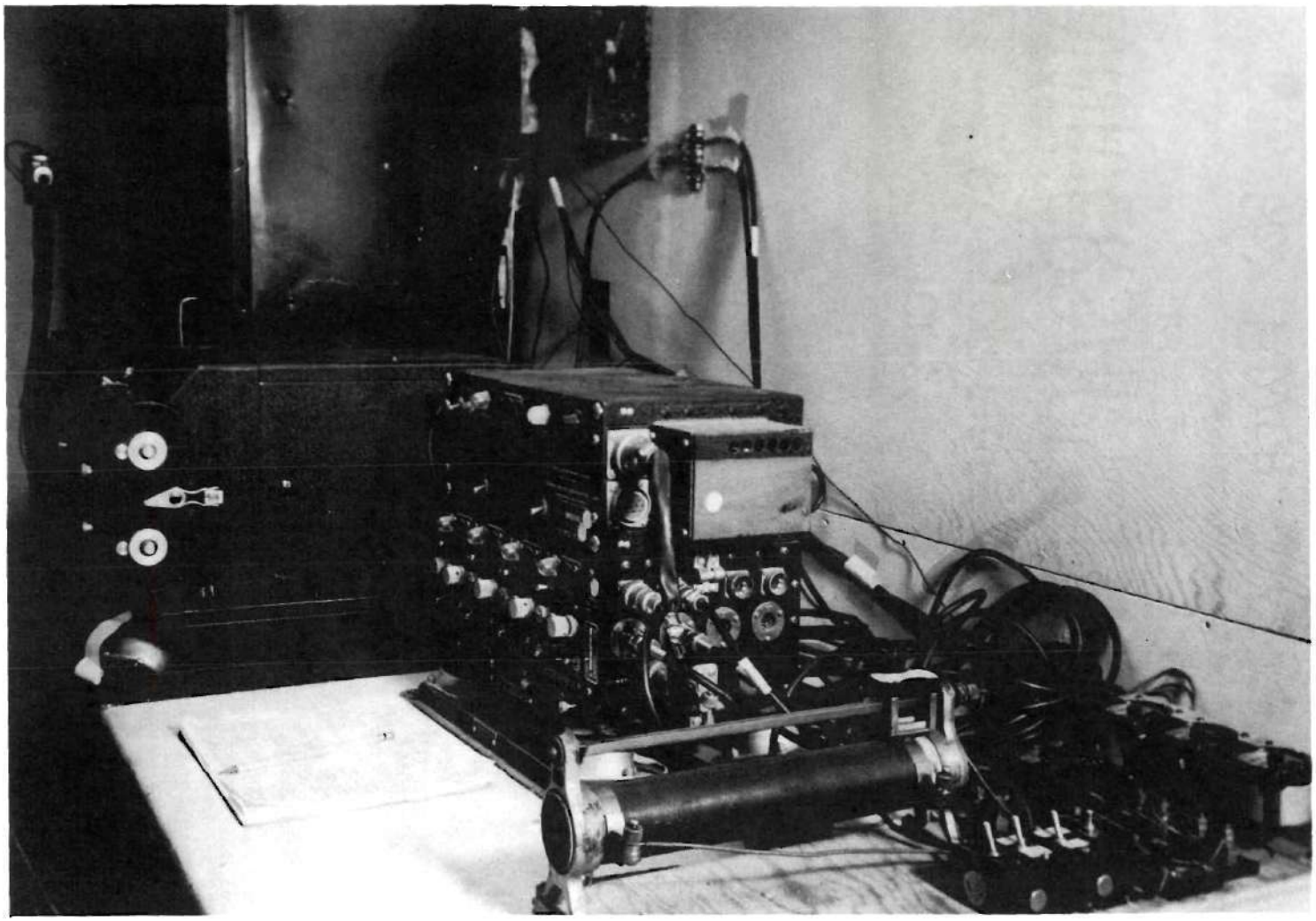

Figure 6. Amplifier, Power Supply and Recording Oscillograph

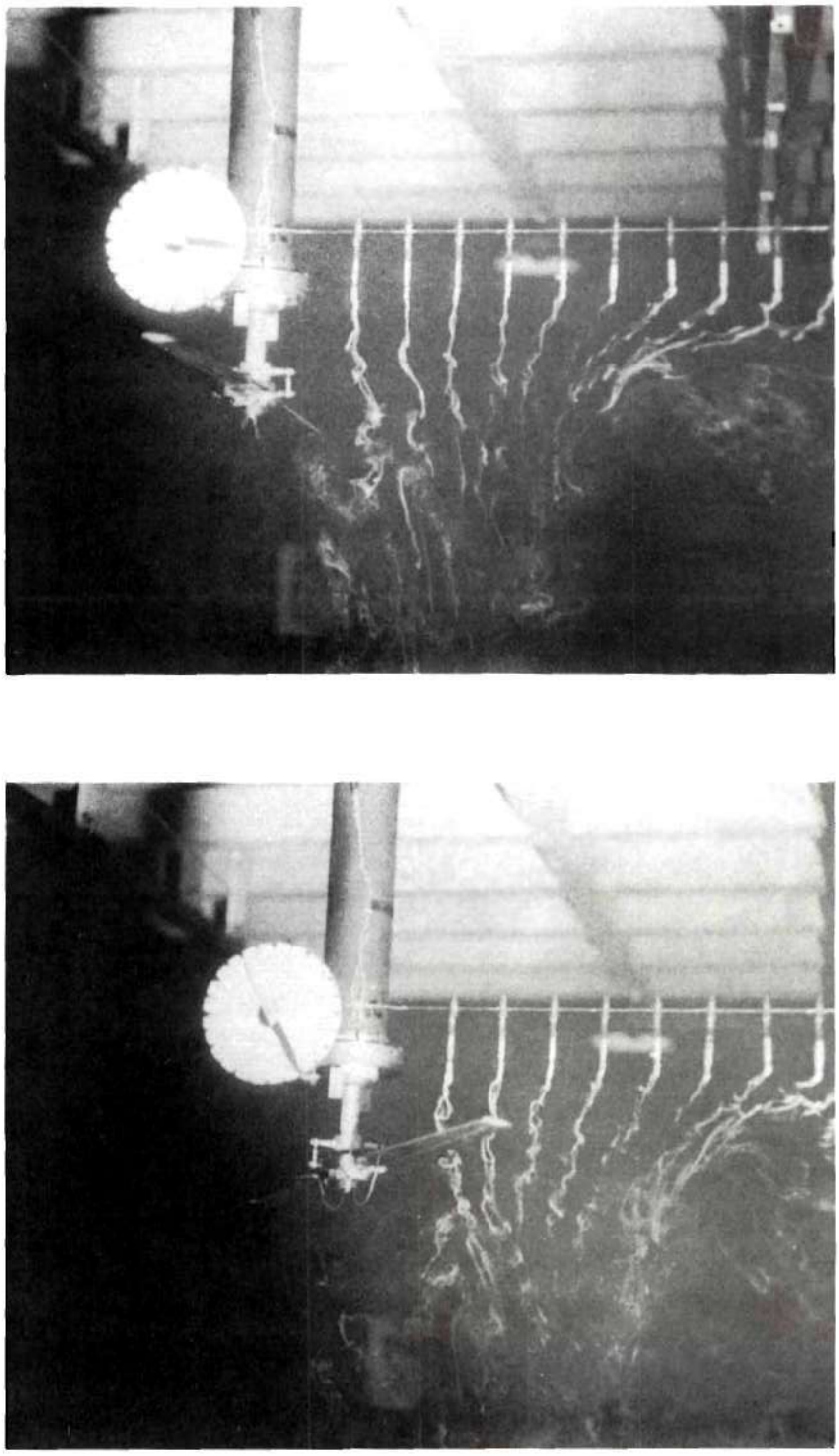

Figure 7. Photographs of the Vortex Sheets in the Wake of a Two-Bladed Hovering Rotor

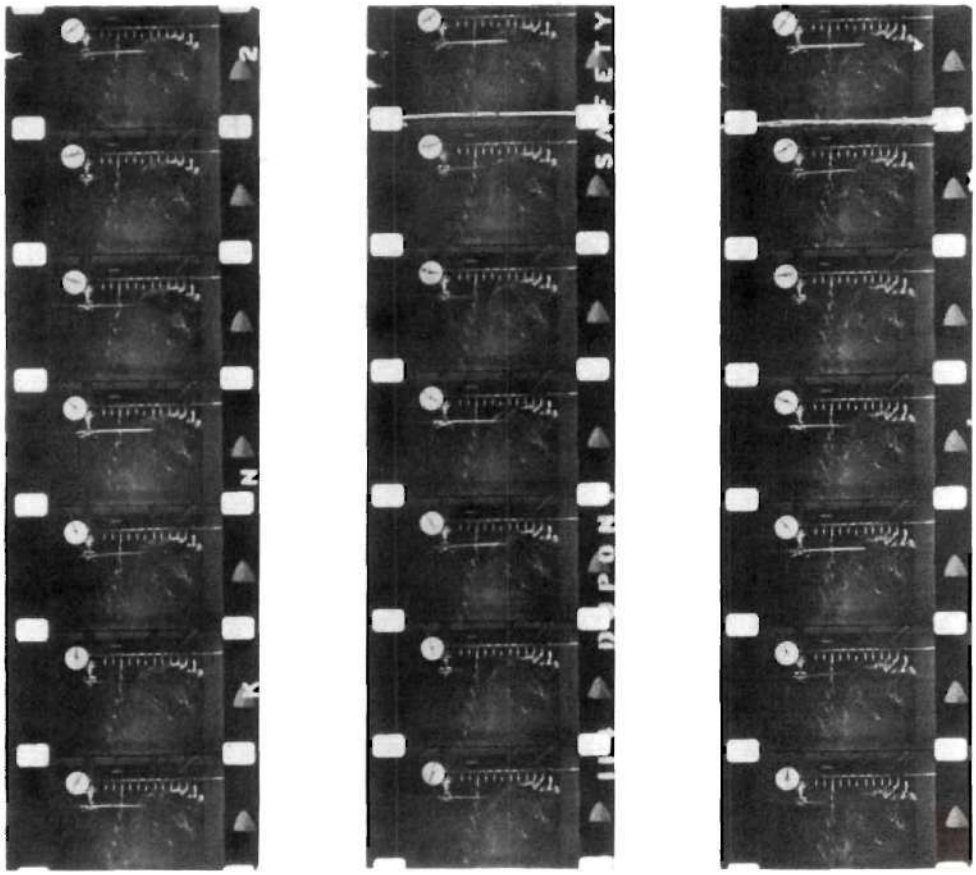

Figure 8. Photographs of the Movement of a Vortex Sheet Element in the Wake of a Two-Bladed Hovering Rotor

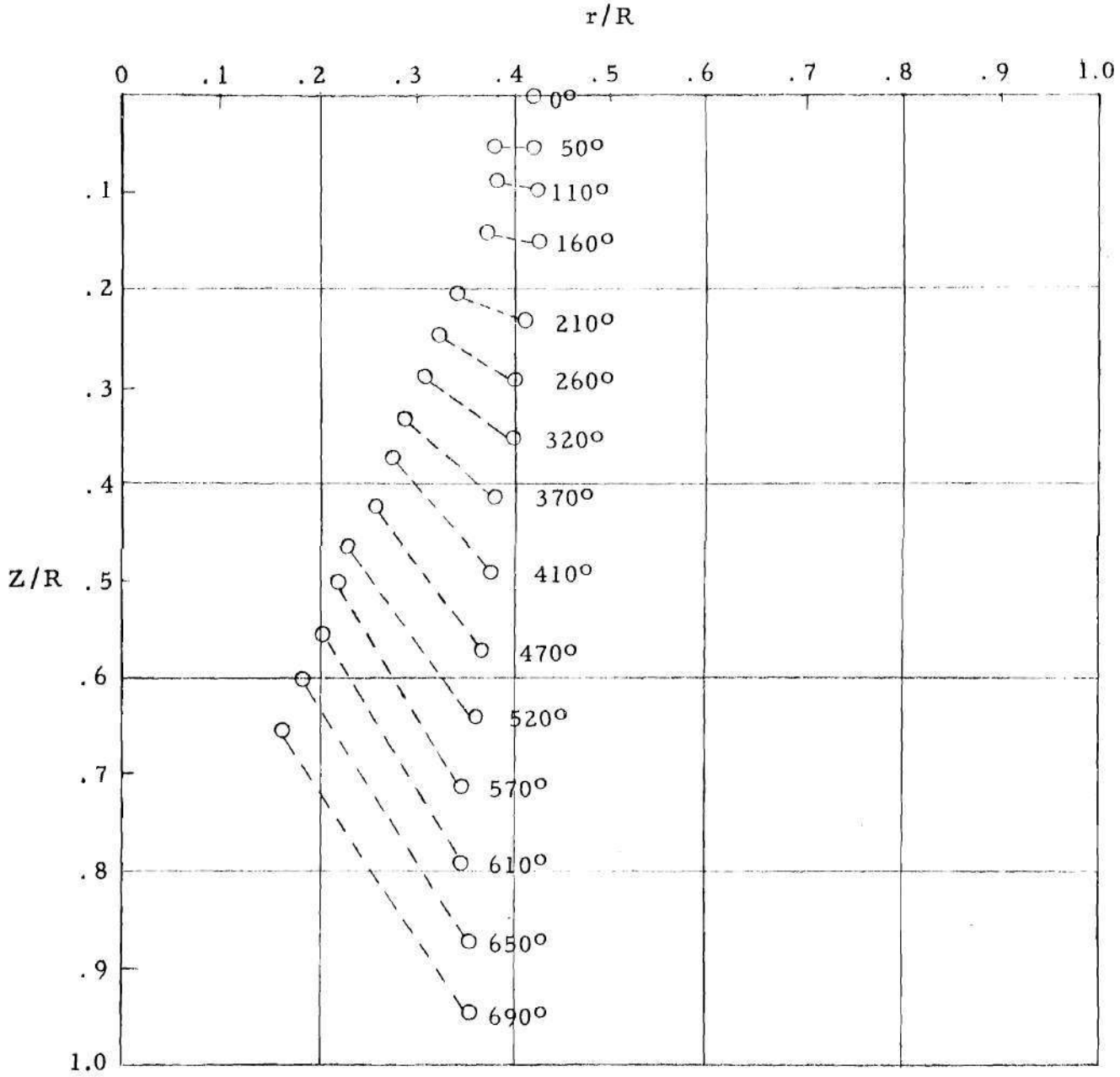

Figure 9. A Typical Plot of the Movement of a Vortex Sheet Element in the Wake of a Two-Bladed Hovering Rotor

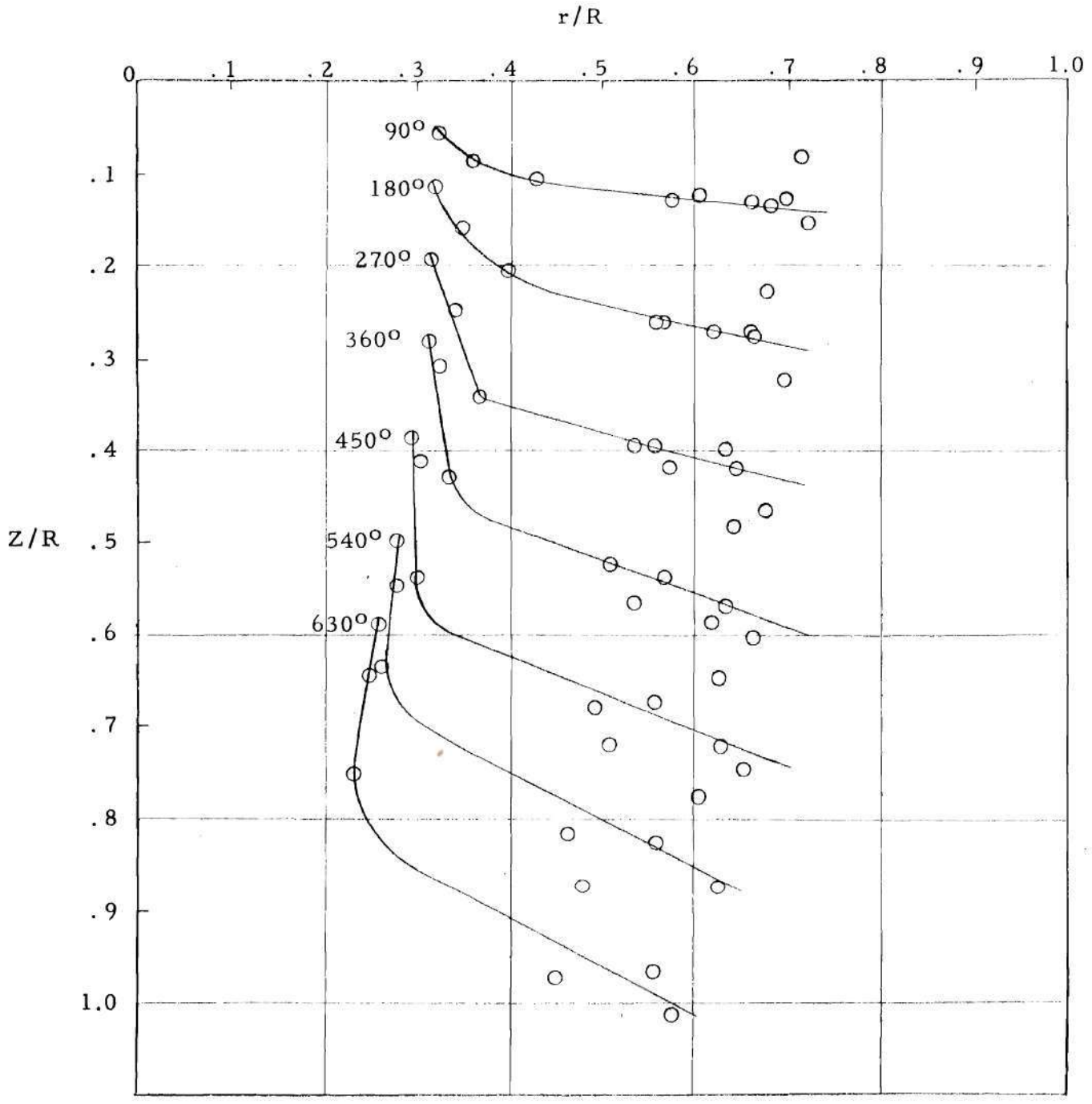

Figure 10. A Plot of the Movement of a Vortex Sheet per 90 degrees of Blade Rotation in the Wake of a Two-Bladed Hovering Rotor

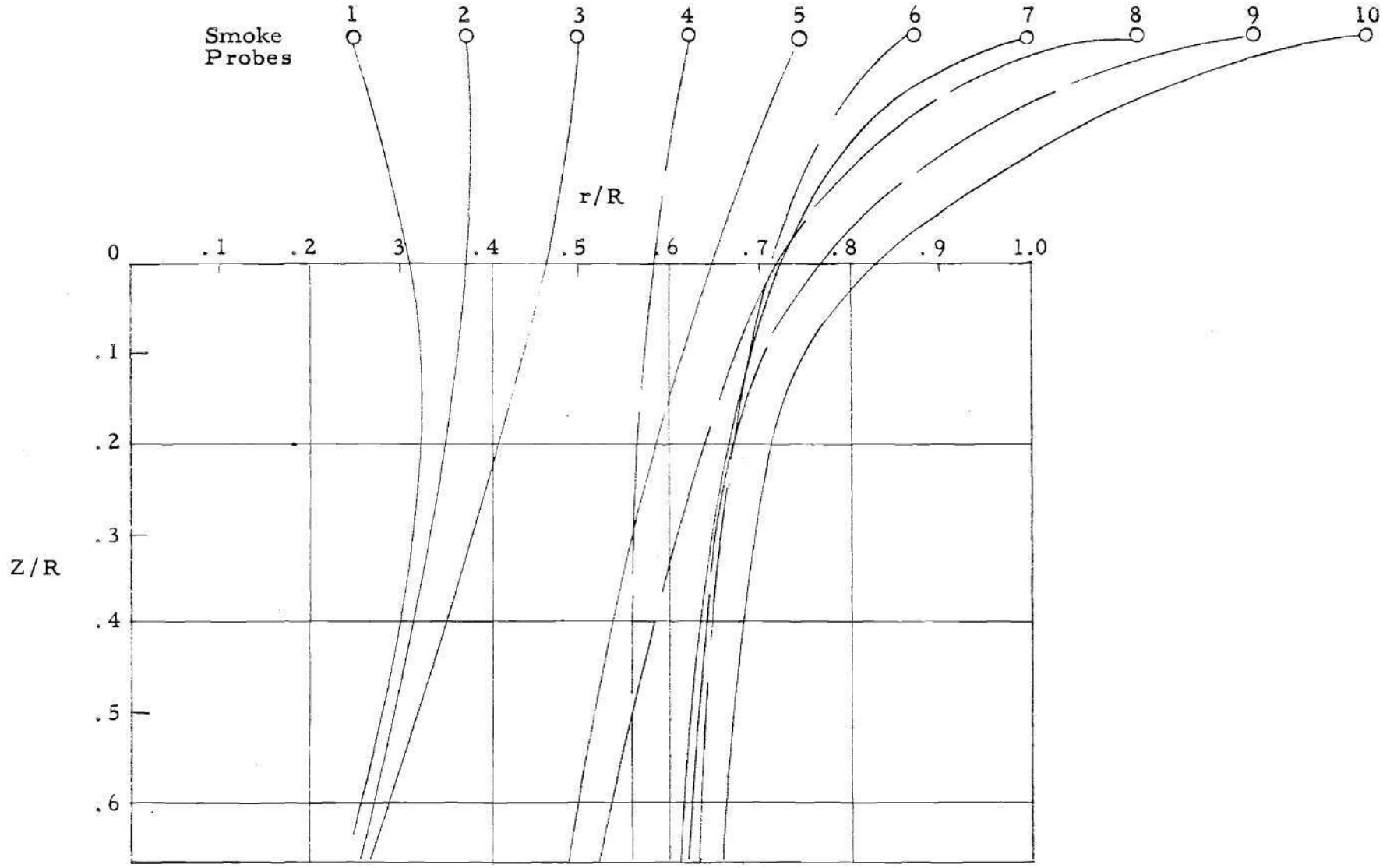

Figure 11. The Paths of the Vortex Sheet Elements in the Wake of a Two-Bladed Rotor

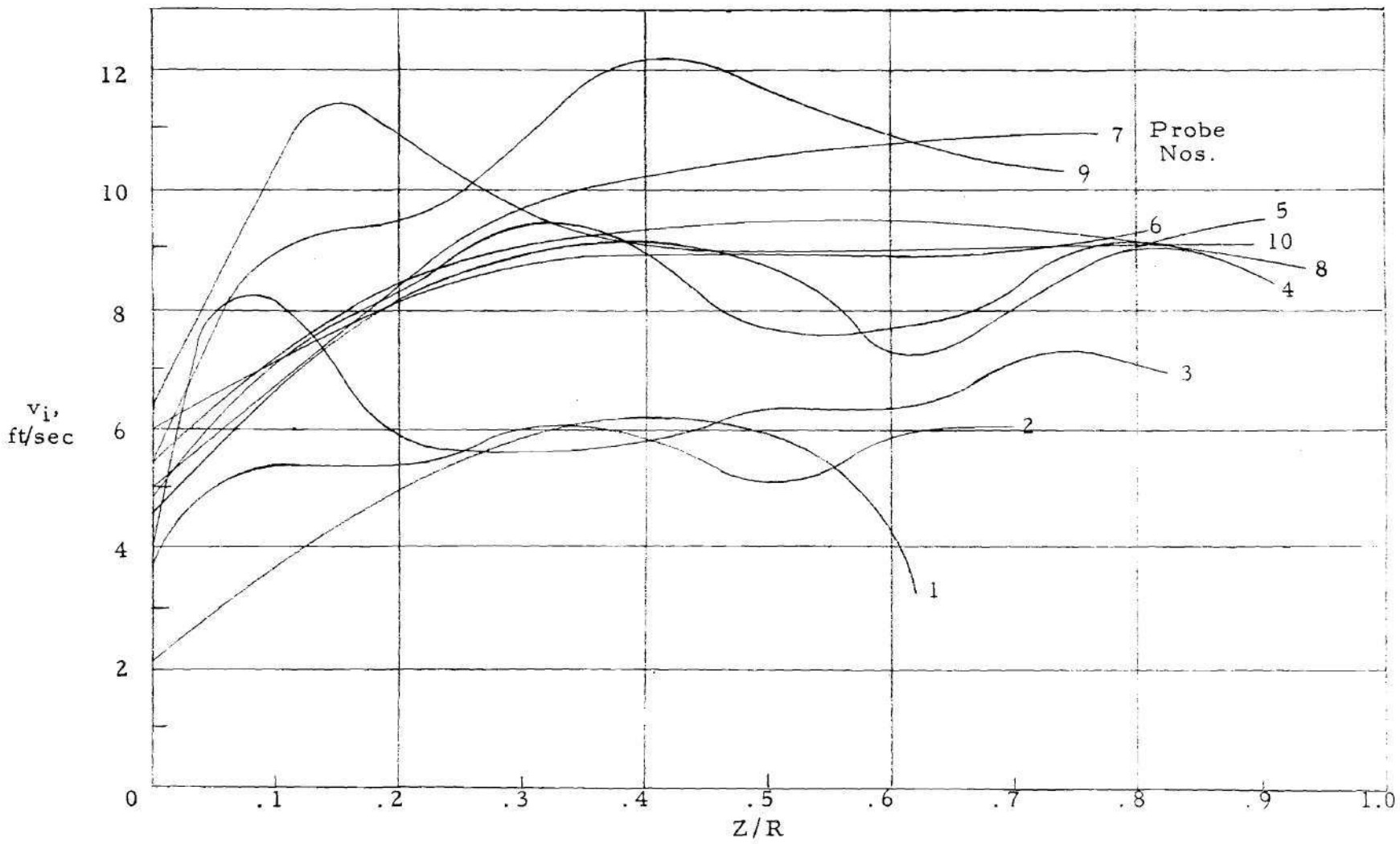

Figure 12. The Average Normal Component of Induced Velocity of the Vortex Sheet Elements in the Wake of a Hovering Two-Bladed Rotor

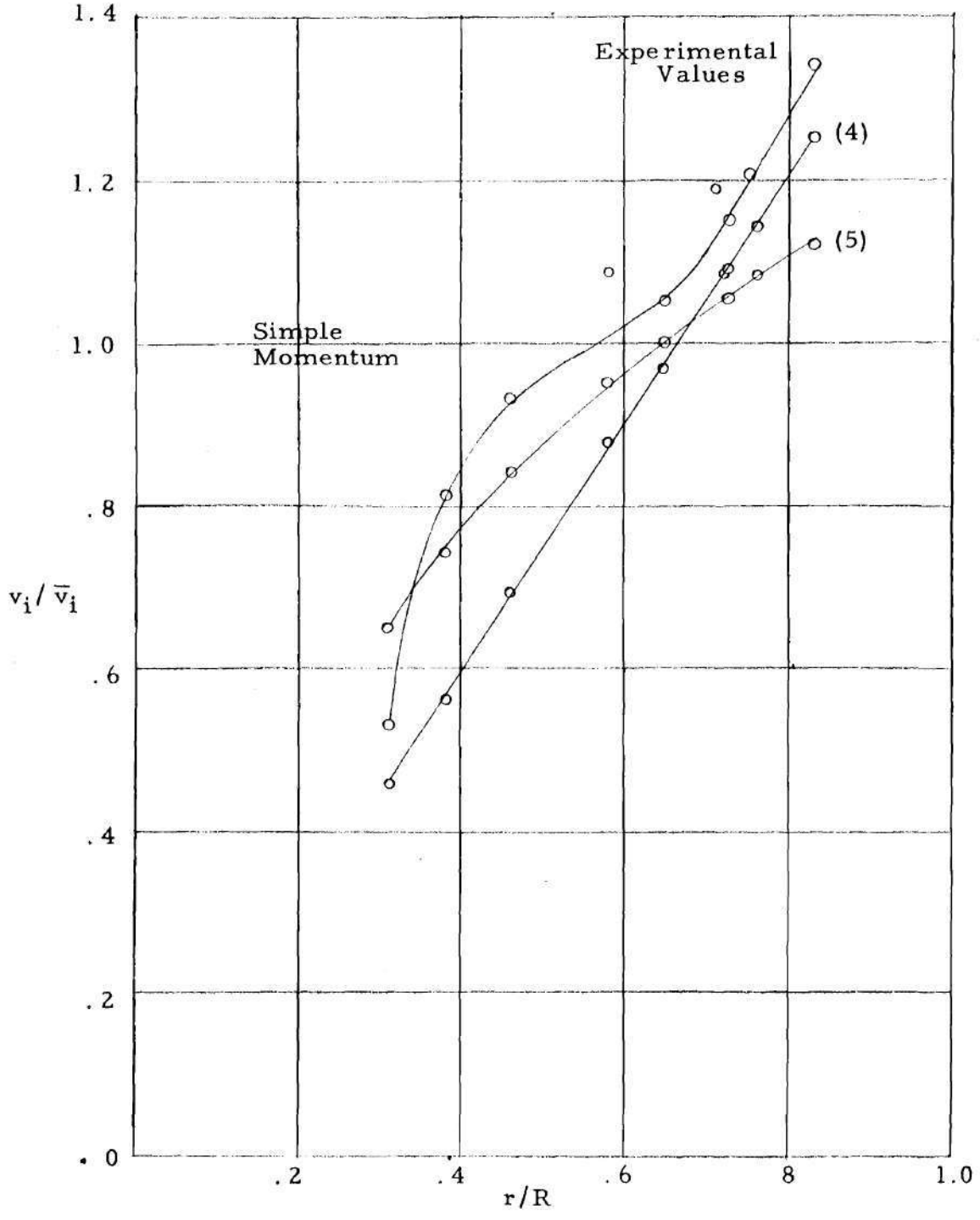

Figure 13. A Comparison of Experimental and Calculated Induced Velocity Ratio $v_i / \bar{v}_i$ in the Plane of the Rotor

BIBLIOGRAPHY

BIBLIOGRAPHY

1. Gray, Robin B., On the Motion of the Helical Vortex Shed from a Single-Bladed Hovering Model Helicopter Rotor and Its Application to the Calculation of the Spanwise Aerodynamic Loading, Princeton University Aeronautical Engineering Department, Report No. 313, 1955.

2. Taylor, Marion K., A Balsa-Dust Technique for Air-Flow Visualization and Its Application to Flow Through Model Helicopter Rotors in Static Thrust, National Advisory Committee for Aeronautics, Technical Note No. 2220, 1950, p. 2.

3. Castles, Walter Jr., Approximate Solution for Streamlines about a Lifting Rotor Having Uniform Loading and Operating in Hovering or Low-Speed Vertical Ascent Flight Conditions, National Advisory Committee for Aeronautics, Technical Note No. 3921, 1957, p. 13.

4. Heyson, Harry H. and Katzoff, S., Normal Component of Induced Velocity in the Vicinity of a Lifting Rotor with a Nonuniform Disk Loading, National Advisory Committee for Aeronautics, Technical Note No. 3690, 1956.

5. Castles, Walter Jr. and Gray, Robin B., Empirical Relation between Induced Velocity, Thrust and Rate of Descent of a Helicopter Rotor as Determined by Wind-Tunnel Tests on Four Model Rotors, National Advisory Committee for Aeronautics, Technical Note No. 2474, 1951.

6. Castles, Walter Jr., The Average Value and Longitudinal Gradient of the Induced Velocity at a Helicopter Rotor Operating at Positive Angles of Attack as Determined by Wind-Tunnel Force Tests of a Four Foot Diameter Model Rotor, Unpublished Report, Engineering Experiment Station of the Georgia Institute of Technology, 1955, p. 31.

7. Jacobs, Eastman N. and Sherman, Albert, Airfoil Section Characteristics as Affected by Variations of the Reynolds Number, National Advisory Committee for Aeronautics, Technical Report No. 586, 1937, p. 27.